The Synthesis and Characterization of 4, 5, and 6 Coordinate Ni(II) Complexes of the "Heteroscorpionate" Ligand (3-*tert*-Butyl-2-hydroxy-5-methylphenyl)bis(3,5-dimethylpyrazolyl)methane

Brian S. Hammes and Carl J. Carrano*

The Department of Chemistry, Southwest Texas State University, San Marcos, Texas 78666

Received January 20, 1999

Six new Ni(II) complexes of the "heteroscorpionate" ligand (3-*tert*-butyl-2-hydroxy-5-methylphenyl)bis(3,5-dimethylpyrazolyl)methane, L1OH, have been prepared and characterized (in most cases crystallographically). These complexes include: tetracoordinate [Ni(L1O)Cl]; pentacoordinate [Ni(L1O)(acac)] and [Ni(L1O)(OAc)]; and hexacoordinate [Ni(L1O)(acac)(pz)], [Ni(L1O)(OAc)(MeOH)], and [Ni(L1O)$_2$]. This second generation of heteroscorpionate ligand supports a tetrahedral environment for Ni(II) but is not a tetrahedral enforcer. Thus the tetra- and pentacoordinate species readily add additional ligands to produce 5- and 6-coordinate complexes. The formation of the undesirable, coordinatively saturated, [Ni(L1O)$_2$], "sandwich" complex is only a minor interference in most of these reactions unlike the situation seen with the previous generation of ligand. This family of heteroscorpionates shows promise as platforms for biomimetic studies which are already underway.

Introduction

Since the initial development of tris(pyrazolyl)borates by Trofimenko and others, these so-called "scorpionate" ligands have found wide application in coordination, organometallic, and bioinorganic chemistry.[1] They are particularly valuable in the biomimetic coordination chemistry of numerous metalloproteins since these monoanionic, facially coordinating ligands have histidine-like donors which can hold three cis sites fixed while leaving other coordination sites open. Despite these advantages, the tris(pyrazolyl)borate ligands are completely symmetric with all nitrogen donors, and many metalloprotein active sites do not have such monofunctional donor spheres. Thus there is a need for polyfunctional ligands which retain the desirable properties of the tris(pyrazolyl)borates.

We and others have therefore embarked on a program for the synthesis of "heteroscorpionate" ligands.[2−7] Our new ligands are related to tris(pyrazolyl)methane, but with one of the pyrazole arms replaced by a phenol, thiophenol, phenylcarboxylic acid or other functionalized aromatic group. Steric hindrance is easily incorporated into the ligands via the pyrazole and/or aromatic rings, giving considerable coordinative flexibility. In all of the ligands we have previously synthesized, the nature of the metal complex formed depended on several factors, including the particular metal involved, the degree of substitution on the pyrazole and aromatic arms, and the ligand-to-metal ratio. Unfortunately, it had only been possible to prepare mononuclear complexes of the type ML$_2$; and also a series of homo- and heterometallic di- and trinuclear species with bridging phenol or thiophenols.[8−13] While these complexes are interesting for their magnetic interactions between metal ions, mononuclear MLX complexes, likely to be of value in modeling metalloprotein sites, have not until now been forthcoming. In this report we describe a new heteroscorpionate ligand (L1OH) (Figure 1) and its Ni(II) complexes where the balance of steric forces allows for the formation of mononuclear MLX species in which the metal can be 4-, 5-, or 6-coordinate. This finally opens the way for the use of these ligands in bioinorganic modeling studies.

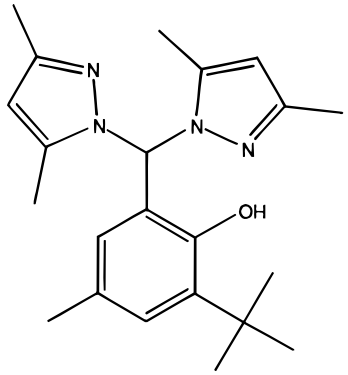

Figure 1. Structure of the ligand used in this study.

Experimental Section

All syntheses were carried out in air and the reagents and solvents were purchased from commercial sources and used as received. The

(1) Trofimenko, S. *Chem. Rev.* **1993**, *93*, 943.
(2) Higgs, T. C.; Carrano, C. J. *Inorg. Chem.* **1997**, *36*, 291.
(3) Higgs, T. C.; Ji, D.; Czernuscewicz, R.; Matzanke, B. F.; Schunemann, V.; Trautwein, A. X.; Helliwell, M.; Ramirez, W.; Carrano, C. J. *Inorg. Chem.* **1998**, *37*, 2383.
(4) Ghosh, P.; Parkin, G. *J. Chem. Soc., Chem. Commun.* **1998**, 413.
(5) Kimblin, C.; Hascall, T.; Parkin, G. *Inorg. Chem.* **1997**, *36*, 5680.
(6) Dowling, C.; Parkin, G. *Polyhedron* **1996**, *15*, 2463.
(7) Ge, P.; Haggerty, B. S.; Rheingold, A. L.; Riordan, C. G. *J. Am. Chem. Soc.* **1994**, *116*, 8406.
(8) Higgs, T. C.; Carrano, C. J. *Inorg. Chem.* **1997**, *36*, 298.
(9) Higgs, T. C.; Ji, D.; Czernuscewicz, R. S.; Carrano, C. J. *Inorg. Chim. Acta* **1998**, *273*, 14.
(10) Higgs, T. C.; Spartalian, K.; O'Connor, C. J.; Matzanke, B. F.; Carrano, C. J. *Inorg. Chem.* **1998**, *37*, 2263.
(11) Higgs, T. C.; Dean, N. S.; Carrano, C. J. *Inorg. Chem.* **1998**, *37*, 1473.
(12) Higgs, T. C.; Ji, D.; Czernuscewicz, R. S.; Carrano, C. J. *Inorg. Chim. Acta* **1999**, *286*, 80.
(13) Higgs, T. C.; Ji, D.; Czernuscewicz, R. S.; Spartalian, K.; Seip, C.; O'Connor, C. J.; Carrano, C. J. *J. Chem. Soc., Dalton Trans.* **1999**, 807.

10.1021/ic9900962 CCC: $18.00 © 1999 American Chemical Society
Published on Web 07/08/1999

ligand precursors, bis(3,5-dimethylpyrazolyl)ketone[2] and 3-*tert*-butyl-2-hydroxy-5-methylbenzaldehyde[14] were prepared using previously reported procedures.

((3-*tert*-Butyl-2-hydroxy-5-methylphenyl)bis(3,5-dimethylpyrazolyl))methane (L1OH). 3-*tert*-Butyl-2-hydroxy-5-methylbenzaldehyde (7.5 g, 39 mmol) was combined with bis(3,5-dimethylpyrazolyl)ketone (8.3 g, 37 mmol) and $CoCl_2 \cdot 6H_2O$ (0.083 g, 1.0 mmol) in a 250 cm^3 round-bottom flask. The mixture was warmed to 120 °C and stirred for 2.5 h, during which time the mixture melted and then resolidified with evolution of CO_2. The resulting blue solid was dissolved in dichloromethane and washed two times with H_2O and once with a saturated solution of NaCl. The organic layer was collected and dried over anhydrous $MgSO_4$. Volatiles were removed under reduced pressure and the crude product slurried with cold pentane. Filtration yielded 9.89 g (71%) of L1OH as a white solid. ^{1}H NMR ($CDCl_3$) δ 9.21 (s, 1 H, O*H*), 7.18 (s, 1H, $-CH-$), 7.13 (d, 1 H, $J = 2$ Hz, Ar*H*), 6.60 (d, 1 H, $J = 2$ Hz, Ar*H*), 5.85 (s, 1 H, Pz*H*), 2.23 (s, 3 H, Ar$-CH_3$), 2.18 (s, 6 H, Pz$-CH_3$), 2.07 (s, 6 H, Pz$-CH_3$), 1.40 (s, 9 H, $-C(CH_3)_3$). ^{13}C NMR ($CDCl_3$) δ 152.28, 148.22, 140.55, 139.32, 129.07, 128.36, 127.93, 123.14, 106.99, 74.63, 34.94, 29.73, 20.97, 13.73, 11.36. Anal. Calcd (found) for L1OH, $C_{22}H_{30}N_4O$: C, 72.09 (71.87); H, 8.27 (8.17); N, 15.28 (15.18).

[Ni(L1O)(Cl)]. A solution of L1OH (0.33 g, 0.89 mmol) in 30 mL of CH_3CN was treated with solid NaOMe (0.048 g, 0.89 mmol) and stirred for 0.5 h. An CH_3CN solution of $NiCl_2 \cdot 6H_2O$ (0.21 g, 0.89 mmol) was added to the reaction mixture. The resulting solution was stirred for 2 h, concentrated under vacuum, and filtered to give a red solid. The red product was treated with dichloromethane and filtered to remove a small amount of white solid (NaCl). The filtrate was concentrated under reduced pressure and crystallized by layering the solution of [Ni(L1O)(Cl)] with isopropyl ether (0.25 g, 61%). Anal. Calcd (found) for [Ni(L1O)(Cl)]·0.25 H_2O, $C_{22}H_{29.5}ClN_4O_{1.25}Ni$: C, 56.92 (56.99); H, 6.36 (6.56); N, 12.06 (11.97). λ_{max} (CH_3OH, ϵ, M^{-1} cm^{-1}): 318 (6000), 414 (sh), 482 (50), 650 (20). λ_{max} (CH_2Cl_2, ϵ, M^{-1} cm^{-1}): 290 (3100), 320 (sh), 426 (340), 544 (270). $\mu_{eff} = 3.49$ μ_B (solid, 298 K).

[Ni(L1O)(OAc)]. A solution of L1OH (0.59 g, 1.6 mmol) in 30 mL of CH_3OH was treated with solid NaOMe (0.088 g, 1.6 mmol). After stirring for 0.5 h, a CH_3OH solution of $Ni(OAc)_2 \cdot 4H_2O$ (0.40 g, 0.89 mmol) was added slowly to the reaction mixture. The resulting solution was stirred for 1 h and concentrated under reduced pressure. The solution was crystallized by slow evaporation of CH_3OH to give 0.44 g (55%) of [Ni(L1O)(OAc)]. Anal. Calcd (found) for [Ni(L1O)(OAc)]·0.5 H_2O, $C_{24}H_{33}N_4O_{3.5}Ni$: C, 58.55 (58.34); H, 6.77 (6.29); N, 11.38 (11.45). FTIR (KBr, cm^{-1}): ν_{CO} (OAc^-) = 1538, 1461. λ_{max} (CH_3OH, ϵ, M^{-1} cm^{-1}): 320 (4500), 386 (sh), 482 (30), 656 (10). λ_{max} (CH_2Cl_2, ϵ, M^{-1} cm^{-1}): 320 (4600), 408 (380), 448 (sh), 712 (30). $\mu_{eff} = 3.64$ μ_B (solid, 295 K).

[Ni(L1O)(acac)]. A solution of L1OH (0.29 g, 0.81 mmol) in 10 mL of CH_3OH was treated with a CH_3OH solution of $Ni(acac)_2$ (0.21 g, 0.81 mmol). The resulting solution was stirred for 1 h and filtered to remove 0.15 g of $Ni(L1O)_2$. Volatiles were removed under reduced pressure to yield 0.16 g (37%) of [Ni(L1O)(acac)]. [Ni(L1O)(acac)] was crystallized by layering a concentrated CH_2Cl_2 solution with isopropyl ether. Anal. Calcd (found) for [Ni(L1O)(acac)]·0.25 H_2O, $C_{27}H_{35.5}N_4O_{3.25}Ni$: C, 61.52 (61.26); H, 6.80 (6.87); N, 11.12 (10.63). FTIR (KBr, cm^{-1}): ν_{CO} (acac) = 1600. λ_{max} (CH_2Cl_2, ϵ, M^{-1} cm^{-1}): 296 (1290), 395 (400), 437 (sh), 642 (20). $\mu_{eff} = 3.15$ μ_B (solid, 298 K).

[Ni(L1O)(acac)(pz)]. A solution of [Ni(L1O)(acac)] (0.096 g, 0.18 mmol) in 10 mL of CH_2Cl_2 was treated with a CH_2Cl_2 solution of 3,5-dimethylpyrazole (0.017 g, 0.18 mmol) and the resulting solution was stirred for 1 h. The CH_2Cl_2 was removed under reduced pressure to give [Ni(L1O)(acac)(pz)] as a green solid which was crystallized by layering a CH_2Cl_2 solution with isopropyl ether to yield 0.059 g (52%). Anal. Calcd (found) for [Ni(L1O)(acac)(pz)], $C_{32}H_{44}N_6O_3Ni$: C, 62.05 (61.87); H, 7.10 (7.07); N, 13.56 (13.52). FTIR (KBr, cm^{-1}): ν_{NH} (pyrazole) = 3384 (m); ν_{CO} (acac) = 1610 (vs). $\mu_{eff} = 2.95$ μ_B (solid, 294 K).

[Ni(L1O)$_2$]. A CH_2Cl_2 solution of [Ni(L1O)(acac)] was layered with isopropyl ether. Over a 4 day period [Ni(L1O)$_2$] crystallized as pale blue blocks, which were filtered off and dried under reduced pressure. Anal. Calcd (found) for [Ni(L1O)$_2$]·0.5H_2O, $C_{44}H_{59}N_8O_{2.5}Ni$: C, 66.16 (66.23); H, 7.46 (7.50); N, 14.03 (13.94). λ_{max} (CH_2Cl_2, ϵ, M^{-1} cm^{-1}): 263 (19560), 329 (12340), 382 (sh). $\mu_{eff} = 3.74$ μ_B (solid, 296 K).

Physical Methods. Elemental analysis on all compounds was performed by Desert Analytics Inc., Tucson, AZ. All samples were dried *in vacuo* prior to analysis. The presence of solvates was corroborated by FTIR, ^{1}H NMR, or X-ray crystallography. ^{1}H and ^{13}C NMR spectra were collected on a Varian UNITY INOVA 400 MHz NMR spectrometer equipped with a Sun workstation. Chemical shifts are reported in ppm relative to an internal standard of TMS. IR spectra were recorded as KBr pellets on a Perkin-Elmer 1600 Series FTIR spectrometer and are reported in wavenumbers. Cyclic voltammetric experiments were conducted using a BAS CV 50W (Bioanalytical Systems Inc., West Lafayette, IN) voltammetric analyzer. All experiments were done under argon at ambient temperature in solutions with 0.1 M tetrabutylammonium hexafluorophosphate as the supporting electrolyte. Cyclic voltammograms (CV) were obtained using a three-electrode system consisting of glassy-carbon working, platinum wire auxiliary, and SCE reference electrodes. The ferrocinium/ferrocene couple was used to monitor the reference electrode and was observed at 0.768 V with $\Delta E_p = 0.120$ V and $i_{pc}/i_{pa} = 1.0$ in CH_2Cl_2 under these conditions. IR compensation was applied before each CV was recorded. Potentials are reported versus the saturated calomel couple. Electronic spectra were recorded using a Hewlett-Packard 8452A diode array spectrophotometer. Room-temperature magnetic susceptibility measurements of the metal complexes were determined using a magnetic susceptibility balance MSB-1 manufactured by Johnson Matthey and calibrated with mercury(II) tetrathiocyanatocobaltate(II) ($\chi_g = 16.44(8) \times 10^{-6}$ cm^3 g^{-1}).[15] Diamagnetic corrections were taken from those reported by O'Connor.[16]

Crystallographic Structure Determination. Crystal, data collection, and refinement parameters for [Ni(L1O)(Cl)]·CH_2Cl_2·H_2O, [Ni(L1O)(OAc)(MeOH)]·2CH_3OH, [Ni(L1O)(acac)], [Ni(L1O)(acac)(pz)], and [Ni(L1O)$_2$]·CH_2Cl_2 are given in Table 1. Crystals of all complexes were sealed in thin-walled glass capillaries. The systematic absences in the diffraction data are consistent with the space groups $P\bar{1}$ for [Ni(L1O)(Cl)]·CH_2Cl_2·H_2O and [Ni(L1O)$_2$]·CH_2Cl_2, $P2_1/n$ for [Ni(L1O)(OAc)(CH_3OH]·2MeOH and [Ni(L1O)(acac)(pz)], and $P2_1/m$ for [Ni(L1O)(acac)(pz)]. The structures were solved using either the Patterson function or direct methods, completed by subsequent difference Fourier syntheses, and refined on F^2 by full-matrix least-squares procedures. All non-hydrogen atoms were refined with anisotropic thermal displacement coefficients, and hydrogen atoms were treated as idealized contributions using a riding model. All software and sources of the scattering factors are those contained in the SHELXTL (5.0) program library (G. Sheldrick, Siemens XRD, Madison, WI).

Results

Synthesis and Reactivity. Reaction of 1 equiv of the deprotonated ligand, $(L1O)^-$, with $NiCl_2$ in a variety of solvents leads to the formation of red-orange solutions from which the desired mononuclear tetrahedrally coordinated Ni(II) species, [Ni(L1O)Cl], is isolated in good to moderate yield. Little or no formation of the coordinatively saturated [Ni(L1O)$_2$] complex was observed. Indeed, attempts to prepare the latter using a 2:1 L/M ratio or employing $Ni(BF_4)_2$ as the metal source were unproductive. This stands in stark contrast to the situation found with our previously investigated heteroscorpionate ligands where the *only* mononuclear species isolated was NiL_2.[2,3,8]

Although a tetrahedral geometry is supported by the ligand $(L1O)^-$, it is not a tetrahedral enforcer and expansion of the

(14) Casiraghi, G.; Casnati, G.; Puglia, G.; Sartori, G.; Terenghi, G. *J. Chem. Soc., Perkin Trans.* **1980**, *1*, 862.

(15) Figgis, B. N.; Nyholm, J. *J. Chem. Soc.* **1958**, 4190.

(16) O'Connor, C. J. *Prog. Inorg. Chem.* **1992**, *29*, 203.

Table 1. Summary of Crystallographic Data and Parameters for [Ni(L1O)(Cl)]·CH_2Cl_2·H_2O, [Ni(L1O)(OAc)(CH_3OH)]·2CH_3OH, [Ni(L1O)(acac)], [Ni(L1O)(acac)(pz)], and [Ni$(L1O)_2$]·CH_2Cl_2

	[Ni(L1O)(Cl)]·CH_2Cl_2·H_2O	[Ni(L1O)(OAc)(CH_3OH)]·2CH_3OH	[Ni(L1O)(acac)]	[Ni(L1O)(acac)(pz)]	[Ni$(L1O)_2$]·CH_2Cl_2
formula	$C_{23}H_{33}Cl_3N_4NiO_2$	$C_{27}H_{44}N_4O_6Ni$	$C_{27}H_{36}N_4NiO_3$	$C_{32}H_{44}N_6NiO_3$	$C_{45}H_{60}Cl_2N_8NiO_2$
fw	562.7	579.5	523.4	619.4	874.7
temp (K)	198(2)	198(2)	198(2)	198(2)	198(2)
cryst syst	triclinic	monoclinic	monoclinic	monoclinic	triclinic
space group	$P\bar{1}$	$P2_1/n$	$P2_1/m$	$P2_1/n$	$P\bar{1}$
cell constants					
a (Å)	9.445(2)	11.0293(12)	9.3065(10)	11.550(3)	9.0923(11)
b (Å)	11.980(3)	19.094(4)	13.397(2)	18.275(4)	9.9158(11)
c (Å)	13.075(2)	13.964(3)	11.157(2)	14.999(4)	13.6838(12)
α (deg)	107.016(12)	90	90	90	74.247(7)
β (deg)	91.42(2)	97.738(11)	105.622(10)	98.59(2)	86.997(11)
γ (deg)	92.58(2)	90	90	90	76.840(9)
Z	2	4	2	4	4
V (Å^3)	1412.0(5)	2914.1(9)	1339.7(3)	3131(2)	1171.3(2)
abs coeff, μ_{calc} (cm^{-1})	10.00	7.01	7.61	6.62	5.73
δ_{calc} (g/cm^3)	1.300	1.129	1.290	1.314	1.240
F(000)	568	1024	546	1320	458
cryst dimens (mm)	0.6 × 0.4 × 0.3	0.7 × 0.7 × 0.7	0.4 × 0.2 × 0.1	0.5 × 0.5 × 0.3	0.4 × 0.2 × 0.2
radiation	Mo Kα (λ = 0.710 73 Å)	Mo Kα (λ = 0.710 73 Å)	Mo Kα (λ = 0.710 73 Å)	Mo Kα (λ = 0.710 73 Å)	Mo Kα (λ = 0.710 73 Å)
h, k, l ranges	−10 → 0, −12 → 12, −14 → 14	−11 → −2, 0 → 20, −13 → 14	0 → 10, −12 → 0, −12 → 11	−10 → 0, −19 → 0, −15 → 16	0 → 8, −10 → 10, −14 → 14
θ range (deg)	1.78−22.50	1.75−22.49	2.27−22.48	1.77−22.50	2.19−22.49
no. of reflens	3674	2327	1830	4020	3098
no. of unique reflens	3407	2327	1713	3786	2867
no. of params	300	347	180	379	232
data/param ratio	11.35	5.71	9.52	9.98	12.36
refinement method	full-matrix least-squares on F^2	full-matrix least-squares of F^2	full-matrix least-squares of F^2	full-matrix least-squares of F^2	full-matrix least-squares of F^2
$R(F)^a$	0.0633	0.0432	0.0492	0.0680	0.0533
$R_w(F^2)^b$	0.1754	0.1198	0.1236	0.1874	0.1282
GOF^c	1.075	1.072	1.026	1.097	1.023
largest diff peak and hole (e/Å^3)	1.113 and −0.460	0.382 and −0.359	0.368 and −0.520	0.825 and −0.940	0.842 and −0.751

[a] $R = [\sum|\Delta F|/\sum|F_o|]$. [b] $R_w = [\sum w(\Delta F)^2/\sum wF_o^2]$. [c] Goodness of fit on F^2.

coordination sphere of the Ni(II) is possible. Thus, reaction of $(L1O)^-$ with $Ni(OAc)_2$ in methanol gives rise to the hexacoordinate species, [Ni(L1O)(OAc)(MeOH)], with a bidentate coordinated acetate. The methanol ligand is, however, very labile, and pumping on the complex results in a rapid color change from blue-green to yellow as the solvent is lost. This presumed pentacoordinate species is also produced (as determined by optical spectroscopy and elemental analysis) upon dissolution of the methanol adduct in noncoordinating solvents such as dichloromethane. Unfortunately, crystals suitable for X-ray diffraction analysis were not forthcoming. Similar behavior is reported for several Ni(II) derivatives of the tris-(3,5-dimethylpyrazolyl)borate homoscorpionate ligand.[17]

Somewhat different behavior is seen when $Ni(acac)_2$ is used as the source of the metal, in which case several products were obtained. If the product was crystallized rapidly from a noncoordinating solvent, the primary species produced was the pentacoordinate [Ni(L1O)(acac)]. However, if the crystallization was slow then two new and unexpected products appeared, both of which are hexacoordinate: [Ni(L1O)(acac)(pz)] and [Ni-$(L1O)_2$]. The former appears to arise from some decomposition of the ligand since there is no free pyrazole in the starting material as determined by NMR. The pyrazole derived from this decomposition is itself a good ligand and occupies the open coordination site in [Ni(L1O)(acac)] producing [Ni(L1O)(acac)-(pz)]. This compound can also be prepared by a rational synthetic route. The [Ni$(L1O)_2$] species appears because the $(acac)^-$ ligand is quite labile in solution and the initial [Ni-(L1O)(acac)] can rearrange to produce small amounts of [Ni-$(L1O)_2$].

$$2[Ni(L1O)(acac)] \rightarrow [Ni(L1O)_2]\downarrow + [Ni(acac)_2]$$

Given enough time, the almost complete insolubility of the latter complex in common organic solvents drives the equilibrium in the direction of what is otherwise a minor product. Thus yellow-green solutions of [Ni(L1O)(acac)] slowly deposit pale blue crystals of [Ni$(L1O)_2$] which eventually account for all of the ligand.

Solid State Structures of the Complexes. The single-crystal X-ray diffraction study on [Ni(L1O)(Cl)], [Ni(L1O)(OAc)-(MeOH)], [Ni(L1O)(acac)], [Ni(L1O)(acac)(pz)], and [Ni-$(L1O)_2$] confirm that $(L1O)^-$, formed by deprotonation of the phenol oxygen in L1OH, binds the nickel as a facially coordinating tridentate ligand. Selected distances and angles for all complexes are given in Table 2, and Figures 2−5 show the thermal ellipsoid diagrams for these complexes. More detailed structural parameters are provided in the Supporting Information.

The molecular structure of the four-coordinate compound [Ni-(L1O)Cl] (Figure 2) confirms the pseudo-tetrahedral geometry around the metal ion. The two pyrazolyl nitrogens and one phenolate oxygen donor of $(L1O)^-$ constitute the trigonal face of the tetrahedron. The N(1)−Ni(1)−N(3) and average N_{pz}−Ni−O(1) bond angles are 91.7(2)° and 98.7(1)°, respectively; both are less than the 109.5° angle expected for idealized tetrahedral geometry due to the relatively small bite angle of the ligand. In all cases the seven-membered chelate ring containing the phenolate oxygen supports the larger internal

(17) Zhang, W.; Liao, S.; Collins, K.; Cleland, W. E. Unpublished.

Table 2. Selected Bond Distances and Angles for [Ni(L1O)(Cl)], [Ni(L1O)(OAc)(CH_3OH)], [Ni(L1O)(acac)], [Ni(L1O)(acac)(pz)], and [$Ni(L1O)_2$][a]

Distance (Å) and angle (deg)	[Ni(L1O)(Cl)]	[Ni(L1O)(OAc) (CH_3OH)]	[Ni(L1O)(acac)]	[Ni(L1O)(acac) (pz)]	[$Ni(L1O)_2$]
Ni(1)−N(1)	1.969(5)	2.042(4)	2.041(4)	2.089(5)	2.075(3)
Ni(1)−N(1)#1			2.041(4)		2.075(3)
Ni(1)−N(3)	1.967(5)	2.028(4)		2.063(5)	2.118(3)
Ni(1)−N(3)#1					2.118(3)
Ni(1)−N(5)				2.140(6)	
Ni(1)−O(1)	1.866(4)	1.979(3)	1.921(4)	1.993(5)	2.048(3)
Ni(1)−O(1)#1					2.048(3)
Ni(1)−O(2)		2.110(4)	1.986(3)	2.051(4)	
Ni(1)−O(3)		2.161(4)	1.986(3)	2.066(5)	
Ni(1)−O(4)		2.109(3)			
Ni(1)−Cl(1)	2.202(2)				
N(1)−Ni(1)-N(3)	91.7(2)	86.6(2)	85.6(2)	87.0(2)	85.35(13)
N(1)−Ni(1)-O(1)	98.1(2)	91.3(2)	96.64(14)	91.1(2)	92.70(12)
N(3)−Ni(1)-O(1)	99.2(2)	92.72(14)	96.64(14)	91.0(2)	91.03(12)

[a] Numbers in parentheses are estimated standard deviations.

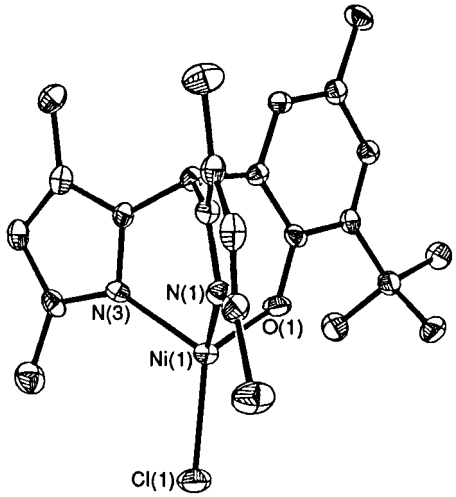

Figure 2. ORTEP diagram with 30% thermal ellipsoids for [Ni(L1O)-Cl] showing atomic labeling for the coordination sphere only.

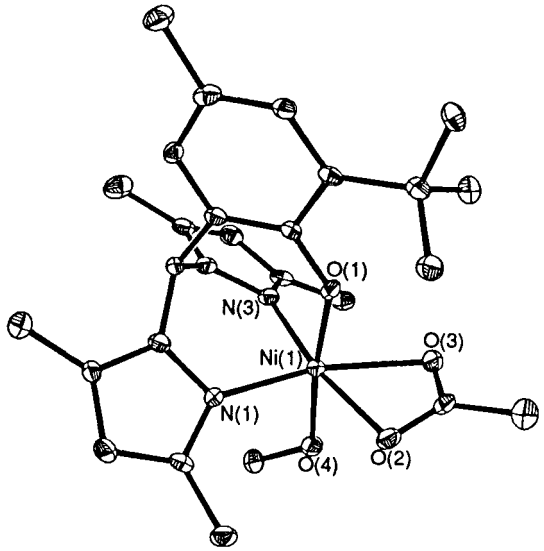

Figure 3. ORTEP diagram with 30% thermal ellipsoids for [Ni(L1O)-(OAc)(MeOH)] showing atomic labeling for the coordination sphere only.

angle. The average Ni(1)−N_{pz} and Ni(1)−O(1) bond distances observed in [Ni(L1O)Cl] are 1.968(4) Å and 1.866(4) Å, respectively, which are, as expected, shorter than those observed in the higher coordination number compounds [Ni(L1O)(OAc)-(MeOH)], [Ni(L1O)(acac)], [Ni(L1O)(acac)(pz)], and [Ni-$(L1O)_2$]. The chloride ion, Cl(1), is positioned perpendicular to the trigonal plane formed by two pyrazolyl nitrogens and one phenolate oxygen with O(1)−Ni^{II}−Cl(1) and average N_{pz}−Ni(1)−Cl(1) bond angles of 122.75(13)° and 119.4(1)°, respectively, and a Ni(1)−Cl(1) bond distance of 2.202 Å. This distance is not unusual and is similar to those reported for other Ni(1)−Cl complexes.[18−22]

The five coordinate complex [Ni(L1O)(acac)], shown in Figure 4a, has a square pyramidal coordination geometry about the Ni(II) ion ($\tau = 0°$)[23] with the two oxygen donors from the $(acac)^-$ and two pyrazolyl nitrogen donors from $(L1O)^-$ forming the equatorial plane. The Ni(II) ion lies slightly above this plane and is displaced 0.18 Å toward the phenolate oxygen, which constitutes the axial donor. The structural analysis also shows a crystallographic plane of symmetry which runs parallel with the plane formed by the aryl ring. The two pyrazolyl nitrogens N(1) and N(1)#1 are positioned trans to the two oxygen donors from the $(acac)^-$ ligand with Ni(1)−N(1) and Ni(1)−N(1)#1 distances of 2.041(3) Å. The axial phenolate oxygen O(1) to Ni(1) bond is 1.921 Å with average O(1)−Ni(1)−N_{pz} and O(1)−Ni(1)−O_{acac} bond angles of 96.64(3)° and 93.55(9)°, respectively. The Ni(1)−O(1) distance in [Ni(L1O)(acac)] is slightly longer than that in the four-coordinate [Ni(L1O)Cl] (Ni(1)−O(1) = 1.866(4) Å) but shorter than that in the six-coordinate complexes [Ni(L1O)(OAc)(MeOH)], [Ni(L1O)(acac)(pz)], and [$Ni(L1O)_2$] (Ni(1)−O(1) = 1.979(3), 1.993(5), and 2.048(3) Å, respectively).

The molecular structures of the six-coordinate [Ni(L1O)-(OAc)(MeOH)] (Figure 3), [Ni(L1O)(acac)(pz)] (Figure 4b), and [$Ni(L1O)_2$] (Figure 5) all have a pseudo-octahedral geometry about the Ni(II) ion with two pyrazolyl nitrogens and a phenolate oxygen from at least one facially coordinating $(L1O)^-$. The average N(1)−Ni(1)−N(3) and N_{pz}−Ni(1)−O(1) angle found for all three complexes ranges from 86.6(2)° and 92.0(7)° for [Ni(L1O)(OAc)(MeOH)] to 87.0(2)° and 91.0(1)° for [Ni(L1O)-(acac)(pz)]. The phenolate oxygens O(1) and O(1)#1 in [Ni-$(L1O)_2$] adopt a trans configuration (O(1)−Ni(1)−O(1)#1 = 180°) with the four pyrazole nitrogens located in a plane. The

(18) Gerloch, M.; Hanton, L. R.; Manning, M. R. *Inorg. Chim. Acta* **1981**, *48*, 205.
(19) Greene, P. T.; Sacconi, L. *J. Chem. Soc.* **1970**, 866.
(20) Jansen, J. C.; Von Koningsveld, H.; Van Ooijen, J. A. C.; Reedijk, J. *Inorg. Chem.* **1980**, *19*, 170.
(21) Masood, M. A.; Hodgson, D. J. *Inorg. Chem.* **1994**, *33*, 3038.
(22) Driessen, W. L.; de Vos, R. M.; Etz, A.; Reedijk, J. *Inorg. Chim. Acta* **1995**, *235*, 127.
(23) Chien, P. C.; Palenik, G. J. *Inorg. Chem.* **1972**, *11*, 816.

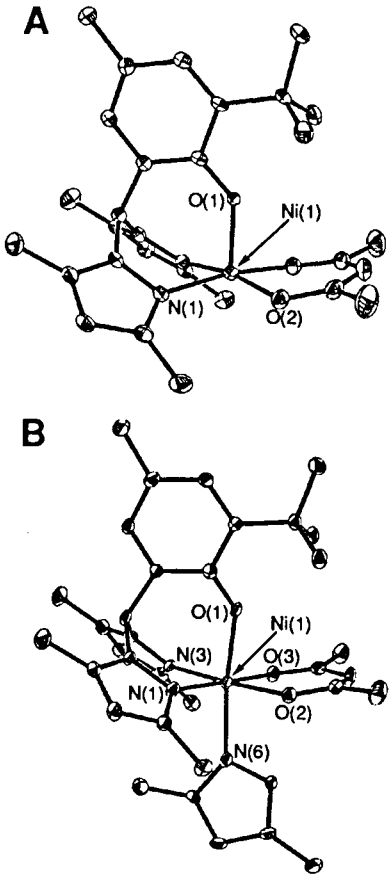

Figure 4. ORTEP diagram with 30% thermal ellipsoids for (A) [Ni(L1O)(acac)] and (B) [Ni(L1O)(acac)(pz)] showing atomic labeling for the coordination sphere only.

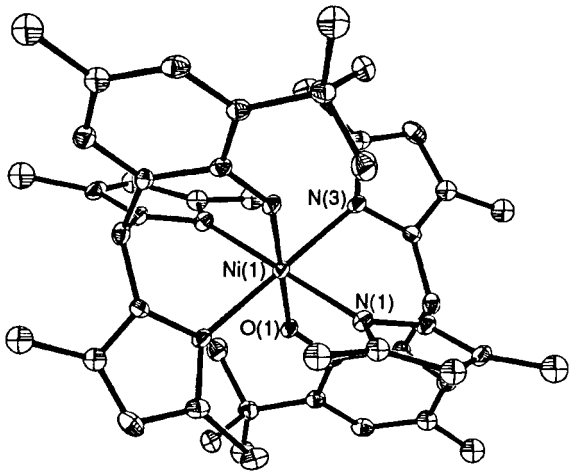

Figure 5. ORTEP diagram with 30% thermal ellipsoids for [Ni(L1O)$_2$] showing atomic labeling for the coordination sphere only.

acetato $(OAc)^-$ ligand in [Ni(L1O)(OAc)(MeOH)] exhibits η^2-coordination to the nickel although with a noticeable asymmetry (Ni(II)−O_{OAc} bond distances: Ni(1)−O(2) = 2.110(4) Å and N(1)−O(3) = 2.161(4) Å).[8,24] In addition, [Ni(L1O)(OAc)(MeOH)] contains a weakly coordinated methanol molecule with a Ni(1)−O(4) bond distance of 2.109(3). The molecular structure of [Ni(L1O)(acac)(pz)] contains $(acac)^-$ and 3,5-dimethylpyrazole ligands in the primary coordination sphere. The $(acac)^-$ is coordinated trans to the pyrazolyl ligands of $(L1O)^-$ with an

(24) Another example of a unsymmetrically coordinated $(OAc)^-$ ligand: Wages, H. E.; Taft, K. L.; Lippard, S. J. *Inorg. Chem.* **1993**, *32*, 4985.

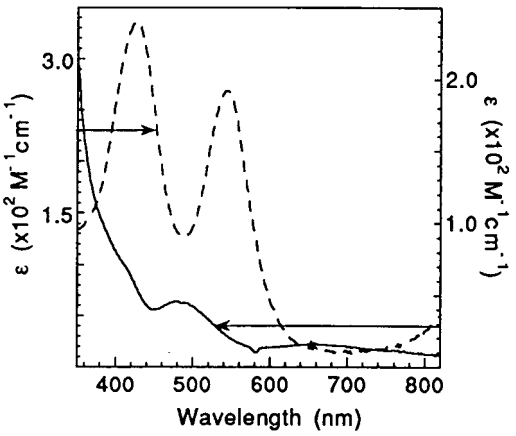

Figure 6. Optical spectra of [Ni(L1O)Cl] in CH_3OH (solid line) and CH_2Cl_2 (dashed line).

average N_{pz}-Ni(1)−O_{acac^-} and O(2)−Ni(1)−O(3) bond angles of 176.8(1)° and 88.9(2)°, respectively. The 3,5-dimethylpyrazole is monodentate and coordinated to the nickel trans to the phenolate oxygen O(1) with a N(6)−Ni(1)−O(1) bond angle of 172.6(2)° and a Ni(1)−N(6) bond distance of 2.140(6) Å. The Ni^{II}−N_{pz} and Ni^{II}−O_{ph} distances observed in [Ni(L1O)(OAc)(MeOH)], [Ni(L1O)(acac)(pz)], and [Ni(L1O)$_2$] are not unusual and are similar to those found for many six-coordinate, high-spin Ni(II) complexes.[2,10,11,18−22]

Electronic Absorption Properties. The electronic absorption spectrum for [Ni(L1O)(Cl)] in CH_2Cl_2 contains two features in the visible region at 426 and 544 nm which have been assigned as the spin-allowed d−d transitions, $^3T_1 \rightarrow {}^3T_1(P)$, and $^3T_1 \rightarrow {}^3A_2$ expected for C_{3v} distorted tetrahedral geometry.[25,26] However, the electronic spectrum of this species in CH_3OH is different and contains three weaker absorption bands in the visible region: a shoulder at 414 nm and two other features at 482 and 650 nm with molecular extinction coefficients of 50 and 20 cm^{-1} M^{-1}, respectively (Figure 6). These band positions and intensities are characteristic of an octahedral coordination environment around a Ni(II) ion and are assigned as $^3A_{2g} \rightarrow {}^3T_{2g}$, $^3A_{2g} \rightarrow {}^3T_{1g}$, and $^3A_{2g} \rightarrow {}^3T_{1g}(P)$ transitions, respectively. The solvent dependence to the optical spectrum of [Ni(L1O)(Cl)] suggests that in coordinating solvents the nickel can add solvent molecules as ligands and thus adopt a higher coordination number.

The visible electronic absorption spectra for [Ni(L1O)(OAc)(CH$_3$OH)] and [Ni(L1O)(acac)] in CH_2Cl_2 both have three features (Figure 7), with a symmetric band at 377 or 395 nm, a shoulder at 448 or 470 nm, and a broad band centered at 712 or 656 nm for [Ni(L1O)(OAc)(CH$_3$OH)] and [Ni(L1O)(acac)], respectively. The similarity of these two spectra suggests that [Ni(L1O)(OAc)(CH$_3$OH)] loses CH_3OH in noncoordinating solvents and that both complexes assume similar pentacoordinate geometries in solution.[27,28] The visible electronic spectrum for [Ni(L1O)(OAc)(CH$_3$OH)] in CH_3OH is very similar to that of [Ni(L1O)(Cl)] in the same solvent, suggesting that a CH_3OH occupies the vacant sites in the latter to form a six-coordinate complex, which is also supported by the crystallographic evidence. Hence, the assignments for these transitions are the

(25) Nicholls, D. In *Comprehensive Inorganic Chemistry*; Bailar, J. C., Emeleus, H. J., Nyholm, R., Trotman-Dickenson, A. F., Eds.; Pergamon Press: Oxford, U.K., 1973; Vol. 3, pp 1152−1159.
(26) Gerloch, M.; Hanton, L. R.; Manning, M. R. *Inorg. Chim. Acta* **1981**, *48*, 205.
(27) Ciampolini, M. *Inorg. Chem.* **1966**, *5*, 35.
(28) Morassi, R.; Bertini, I.; Sacconi, L. *Coord. Chem. Rev.* **1973**, *11*, 343.

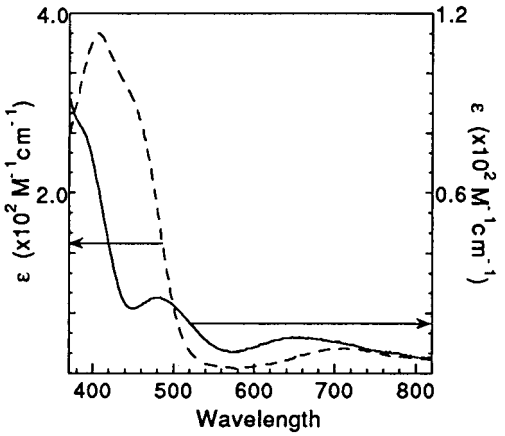

Figure 7. Optical spectra of [Ni(L1O)(OAc)] in CH_3OH (solid line) and CH_2Cl_2 (dashed line).

Table 3. Electrochemical Properties[a] of [Ni(L1O)(Cl)], [Ni(L1O)(OAc)(CH_3OH)], [Ni(L1O)(acac)], [Ni(L1O)(acac)(pz)], and [Ni(L1O)$_2$]

complex	$E_{1/2}$ (V)	ΔE_p (V)	i_c/i_a	$E_{p,a}$ (V)
[Ni(L1O)(Cl)]	0.77	0.17	1.0	0.86
[Ni(L1O)(acac)]	0.58	0.15	0.77	0.66
[Ni(L1O)(OAc)(CH_3OH)]	0.59	0.33	0.78	0.76
[Ni(L1O)(acac)(pz)][b]	0.35	0.12	0.47	0.42
[Ni(L1O)$_2$][c]				

[a] In CH_2Cl_2 at a scan rate of 0.10 V s^{-1}. [b] In the presence of excess 3,5-dimethylpyrazole. [c] Electrochemistry was not done due to a lack of solubility.

same as above for an octahedral system. The visible spectrum of [Ni(L1O)(acac)(pz)] in CH_2Cl_2 indicates the presence of an equilibrium between the six-coordinate complex, [Ni(L1O)(acac)(pz)] and the five-coordinate [Ni(L1O)(acac)].

$$[Ni(L1O)(acac)] + pz \rightleftharpoons [Ni(L1O)(acac)(pz)]$$

The complex [Ni(L1O)$_2$] is so insoluble in all organic solvents that no visible absorption spectrum is obtainable.

Electrochemical Properties. Magnetic susceptibility measurements confirm that the oxidation state of the metal in all the complexes is Ni(II). We have investigated the redox properties of these Ni(II) complexes by cyclic and square wave voltammetry. The results of the cyclic voltammetry (CV) experiments are summarized in Table 3. The cyclic voltammograms for the [Ni(L1O)(Cl)], [Ni(L1O)(acac)], [Ni(L1O)(OAc)(MeOH)], and [Ni(L1O)(acac)(pz)] in CH_2Cl_2 between 1.5 and -1.5 V are all similar with one quasi-reversible oxidation wave observed near $+0.7$ V. Repeated scans between 1.2 and 0.0 V showed no reduction in current for [Ni(L1O)(Cl)], but a gradual decrease in current for [Ni(L1O)(acac)], [Ni(L1O)(OAc)(MeOH)], and [Ni(L1O)(acac)(pz)], demonstrating the lower reversibility of the latter three complexes. However, at faster scan rates ($\nu = 1$ V s^{-1}) ΔE_p for [Ni(L1O)(Cl)] increases, suggesting that even this species is not strictly reversible. The oxidative process in all four systems can be assigned as a ligand- rather than metal-based oxidation by comparison with [Zn(L1O)(Cl)] which also shows a quasi-reversible wave at a similar potential.[29] In addition, the more soluble "sandwich" complex, [Ni(L)$_2$], {where L = (3-*tert*-butyl-2-hydroxy-5-methylphenyl)-bis(pyrazolyl)methane}, shows two closely spaced waves at similar potentials, reinforcing the assignment of these features as ligand based processes. Attempts to isolate the oxidized product of [Ni(L1O)(Cl)] *via* controlled-potential coulometry was unsuccessful due to decomposition of the metal complex over the course of the experiment; but likely it contains a phenoxy radical coordinated to the Ni(II) center as described for similar ligands by Wieghardt *et al.*[30−32]

(29) Hammes, B. S.; Carrano, C. J. *Inorg. Chem.*, submitted.

Discussion

Although it was not the purpose of this work to produce biomimetic Ni(II) complexes, it is interesting to note that [Ni(L1O)(acac)(pz)] is a structural model for the Ni(II) substituted Zn endopeptidase, astacin.[33] The X-ray structures of the native Zn(II) and the substituted Cu(II), Co(II), Ni(II) and Hg(II) species are all available and show that the catalytically *active* Zn, Co, and Cu species adopt a distorted trigonal bypyramidal geometry with an N_3O_2 donor set derived from histidine, tyrosine, and water ligands.[34] The catalytically *inactive* Ni(II) species is six coordinate with an N_3O_3 donor sphere and a distorted octahedral geometry. The inactivity of the Ni(II) species has been attributed to its tendency to expand its coordination sphere to give octahedral species by adding additional ligands (i.e., a second water molecule in the case of the protein), a tendency reproduced by the Ni(II) complexes of both the homo- and heteroscorpionate ligands. The protein structure shows two cis oriented water molecules and two histidine nitrogens making up the equitorial plane; with the tyrosine phenolate oxygen and another histidine nitrogen trans to each other in the axial positions. In the case of [Ni(L1O)(acac)(pz)] the two cis water molecules are replaced by the cis oxygens of the $(acac)^-$ but otherwise the coordination spheres are nearly identical. The most notable difference between the two structures is that the Ni(II)$-O_{ph}$ distance in [Ni(L1O)(acac)(pz)] is the shortest bond in the molecule at 1.99 Å while in the protein it is a rather long 2.3 Å, suggesting a much weaker interaction in the latter. The weak interaction between the phenolate donor and the Ni(II) in the protein is manifested in the so-called tyrosine switch mechanism operative in the serralysins which show that the tyrosine bound to Zn in the resting enzyme is displaced by an incoming substrate or inhibitor.[33]

Finally it should be noted that the primary significance of this work lies, not in the uniqueness of the Ni(II) complexes we describe herein, or in their use as models for Ni(II) substituted proteins, but rather in the development of a heteroscorpionate ligand with adequate steric bulk to stabilize mononuclear, pseudo-tetrahedral, MLX species. At the same time the chelate is of sufficient flexibility to allow for an expansion of the metal coordination sphere upon the addition of small endogenous ligands. Previous work from our group had demonstrated that substituent groups at the 3 and/or 5 position of the pyrazole rings are required to prevent formation of the coordinatively saturated, ML_2 complexes; and we anticipated, based on well-established tris(pyrazolyl)borate chemistry, that the isopropyl or *tert*-butyl substituents would provide a sufficient degree of steric bulk to allow for the

(30) Sokolowski, A.; Adam, B.; Weyermueller, T.; Kikuchi, A.; Hildenbrand, K.; Schnepf, R.; Hildenbrandt, P.; Bill, E.; Wieghardt, K. *Inorg. Chem.* **1997**, *36*, 3702.
(31) Sokolowski, A.; Mueller, J.; Weyermueller, T.; Schnepf, R.; Hildenbrandt. P.; Hildenbrand, K.; Bothe, E.; Wieghardt, K. *J. Am. Chem. Soc.* **1997**, *119*, 8889.
(32) Schnepf, R.; Sokolowski, A.; Mueller, J.; Weyermueller, T.; Bachler, V.; Wieghardt, K.; Hildenbrandt, P. *J. Am. Chem. Soc.* **1998**, *120*, 2352.
(33) Lipscomb, W. N.; Straeter, N. *Chem. Rev.* **1996**, *96*, 2375.
(34) Gomis-Ruth, F.; Grams, F.; Yiallouros, I.; Nar, H.; Kuesthardt, U.; Zwilling, R.; Bode, W.; Stoecker, W. *J. Biol. Chem.* **1994**, *269*, 17111

formation of MLX species. However, use of the isopropyl group as a pyrazole substituent, while preventing coordinatively saturated $M(L)_2$ formation, triggered the development of polynuclear species due to the proclivity for bridging by the pendent phenol or thiophenols, indicating the need for steric protection on the aromatic portion of the ligand as well. Still larger pyrazole substituents such as the *tert*-butyl group seemed to produce such a congested metal center that no complexes could be isolated at all. We now find that the combination of 3,5-dimethyl substitution on the pyrazole and *tert*-butyl at the 3-position of the phenyl rings seems to be the ideal compromise. In addition, the solubility properties of this ligand render it or its derivatives very easy to synthesize in pure form (100 g quantities are easily prepared from commercial materials in as few as two steps) and their metal complexes are usually crystalline. An example of the use of these new ligands for the formation of biomimetic Zn(II) complexes is described in a companion publication. It should be noted that such chemistry was not possible with the previous generations of heteroscorpionates.

Acknowledgment. This work was supported by Grants AI-1157 from the Robert A. Welch Foundation and CHE-9726488 from the NSF. The NSF-ILI program grant USE-9151286 is acknowledged for partial support of the X-ray diffraction facilities at Southwest Texas State University.

Supporting Information Available: A complete list of atomic positions, bond lengths and angles, anisotropic thermal parameters, hydrogen atom coordinates, data collection and crystal parameters, and ORTEP diagrams for all crystallographically characterized complexes are available. This material is available free of charge via the Internet at http://pubs.acs.org.

IC9900962